Self Image Rectification for Uncalibrated Stereo Video with Varying Camera Motions and Zooming Effects

Chia-Ming Cheng[1] Shang-Hong Lai[1] Shyh-Haur Su[2]
Department of Computer Science, National Tsing Hua University, Taiwan[1]
Industrial Technology Research Institute, Taiwan[2]

Abstract

In this paper, we propose a novel self image rectification algorithm for uncalibrated stereo video sequences. Different from conventional stereo systems, this algorithm performs adaptive calibration that allows unequal motions and zooming effects in both cameras. For the first stereo frame, we estimate a reduced set of camera parameters through a nonlinear optimization process to minimize the geometric errors of the corresponding points in pre-rectified image coordinates. For the subsequent frames, these parameters are updated via minimizing the objective function that jointly considers the geometric errors and the smoothness constraints over temporal variations. The experimental results of applying this algorithm to two real sequences are shown to demonstrate its superior performance in reliable rectification distortions and robustness against outliers.

1. Introduction

In stereo matching, image rectification simplifies the search of match points between binocular images in 1D space constrained by the epipolar geometry, so as to search along the corresponding horizontal scanline. Traditional stereo systems assume fixed camera parameters that can be obtained through a careful camera calibration procedure in advance, thus the rectification becomes a subordinate procedure based on a Euclidean transformation up to the camera parameters. However, modern devices and applications, such as pan/tilt cameras, autostereoscopic displays, and robot vision systems, may encounter the case of uncalibrated cameras or varying camera motions or zooming in/out effects, which reveals the demand and importance of capability to calibrate cameras and rectify images from image content itself.

Previous methods that aim to rectify images for stereo matching automatically from images can be roughly classified into two approaches. The first approach, known as *camera self-calibration* [1-4], estimates the camera parameters from a set of match points extracted from the content of input frames. This approach starts with projective or affine reconstruction, and then upgrades to metric reconstruction that is constituted by the physical camera parameters. Finally, the image rectification is performed in the same manner of the calibrated case. Representative techniques for metric upgrade include Kruppa equation [3] and Absolute Dual Quadric (ADQ) [4]. More details can be found in [1,5]. However, the main drawbacks of such methods suffer from the over-fitting problem on projective space, and the projective errors may lead to unreasonable camera parameters which result in unexpected distortion in image rectification.

Figure 1. The left image #0, #60, #180 of the *walk away* stereo sequence with varying camera motion and zooming effect: the first row are original input images, the second row shows the results of projective rectification [6], and the third row shows the rectified images by using the proposed image rectification algorithm.

The other approach, known as *projective rectification* [6,7], rectifies images based on the two-view epipolar geometry, i.e. fundamental matrix, regardless of the Euclidean camera parameters. From the estimated epipolar geometry, the standard process follows three steps: 1) to send the epipole to infinity, 2) to establish the rectification matrices for both images, and 3) to reduce the image distortion while preserving the rectification properties. The main advantage of this approach is that it directly generates the rectified images for stereo matching. However, the aforementioned over-fitting problem in projective space is still unresolved. In addition, the lack of physical meaning in the projective reconstruction makes it difficult to impose meaningful temporal constraint for video sequences.

Among the projective rectification techniques, a series of researches started by Isgro and Trucco [8], followed by Fusiello and Irsara [9], are closely related to this paper. In [8], the authors derived the specific class of rectification homographies by exploiting the fact that the fundamental matrix of a pair of rectified images has a particular form [6], so as to set up a minimization directly from image correspondences without requiring explicit computation of the epipolar geometry. Instead of parameterization directly in the homography matrices, the authors of [9] associate a reduced set of physical

camera parameters with the rectification homography, which results in a so-called quasi-Euclidean rectification. The main difference between their algorithms and the proposed algorithm is that we improve the parameterization with a local optimization to avoid ambiguous solutions and undesirable rectification distortion. Moreover, the robust estimator is employed into the optimization process to overcome the inevitable outlier problem in the feature point correspondence. Lastly, we impose the temporal constraints in the updated image rectification for stereo video sequences.

Our algorithm aims to calibrate cameras as well as rectify images for uncalibrated stereo video sequences with temporally varying camera motions and zooming in/out effects. For the first frame, we estimate a reduced set of camera parameters through a nonlinear optimization process to minimize the geometric errors of the match points in pre-rectified image coordinates. For the subsequent frames, we formulate an objective function that jointly considers the geometric errors and smoothness constraints over temporal variations, and the camera parameters are updated so as to minimize the objective function. In this framework, the proposed algorithm contains the following advantages: 1) temporal stability while varying camera parameters, 2) retainable rectification distortion, and 3) robustness against outliers.

2. Preliminary Background

In this section, we briefly describe the relevant theoretical background for image sectification [6,8,9].

Let ($\mathbf{P}_{ol}$, $\mathbf{P}_{or}$, $\mathbf{P}_{nl}$, $\mathbf{P}_{nr}$) denote the original left, origin right, new left, and new right projection matrices, respectively. The relation between the original and new projection matrices in terms of the rectification homography $\mathbf{H}$ can be written as $\mathbf{P}_n$=$\mathbf{H}\mathbf{P}_o$. For the metric projection matrix, represented as $\mathbf{P}$=$\mathbf{K}[\mathbf{R}^{\mathrm{T}} \mid -\mathbf{R}^{\mathrm{T}}\,\mathbf{t}]$, where $\mathbf{K}$, $\mathbf{R}$, and $\mathbf{t}$ denotes the calibration matrix, rotation matrix, and translation vector, respectively, the rectification homography can be written as follows:

$$\mathbf{H} = \tilde{\mathbf{P}}_n \tilde{\mathbf{P}}_o^{-1} = \mathbf{K}_n \mathbf{R}_n \mathbf{R}_o^{-1} \mathbf{K}_o^{-1} = \mathbf{K}_n \mathbf{R}' \mathbf{K}_o^{-1} \qquad (1)$$

where $\tilde{\mathbf{P}}$ denotes the left 3×3 sub-matrix of $\mathbf{P}$ and $\mathbf{R}' = \mathbf{R}_n \mathbf{R}_o^{-1}$ is the combined rotation matrix. Based on the two-view epipolar geometry, i.e. $\mathbf{m}_r{}^T\mathbf{F}\mathbf{m}_l$=0 for a pair of corresponding image points ($\mathbf{m}_l$, $\mathbf{m}_r$) and $\mathbf{F}$ is the associated fundamental matrix, this linear constraint on the rectified image coordinates can be formulated as:

$$\left(\mathbf{H}_r \mathbf{m}_r^j\right)^T [\mathbf{u}_1]_\times \left(\mathbf{H}_l \mathbf{m}_l^j\right) = 0 \qquad (2)$$

where the 3-vector $\mathbf{u}_1 = (1,0,0)^T$, and $[\ ]_\times$ denotes a 3×3 skew symmetric matrix defined as a cross product operator of two 3-vectors, i.e. $[\mathbf{a}]_\times \mathbf{b} = \mathbf{a}\times\mathbf{b}$ [1], the index *r* and *l* denote the right and left images, and the index j denotes the *j*-th pair of correspondence points. Note that $[\mathbf{u}_1]_\times$ is a specific form of the fundamental matrix for a rectified image pair. In [6], the authors used equation (2) as the objective function, parameterized by $\mathbf{H}_r$ and $\mathbf{H}_l$ with 10 d.o.f (2 for $\mathbf{H}_r$ and 8 for $\mathbf{H}_l$), for the cost minimization on manually selected match points.

From equation (1) and (2), the fundamental matrix can be re-written as follows:

$$\begin{aligned}\mathbf{F} &= \mathbf{H}_r^T [\mathbf{u}_1]_\times \mathbf{H}_l \\ &= \mathbf{K}_{or}^{-T} \mathbf{R}_{or}^{-T} \mathbf{R}_{nr}^T \mathbf{K}_{nr}^T [\mathbf{u}_1]_\times \mathbf{K}_{nl} \mathbf{R}_{nl} \mathbf{R}_{ol}^{-1} \mathbf{K}_{ol}^{-1} \\ &= \mathbf{K}_{or}^{-T} \mathbf{R}_r'^T \mathbf{K}_{nr}^T [\mathbf{u}_1]_\times \mathbf{K}_{nl} \mathbf{R}_l' \mathbf{K}_{ol}^{-1}\end{aligned} \qquad (3)$$

Note that the calibration matrix $\mathbf{K}$ has 5 d.o.f. and the combined rotation matrix $\mathbf{R}' = \mathbf{R}_o \mathbf{R}_n^T$ has 3 d.o.f. In this formulation, the fundamental matrix is parameterized in terms of the metric camera matrices. In [9], the authors showed that $\mathbf{K}_{nr}^T [\mathbf{u}_1]_\times \mathbf{K}_{nl}$ equals (up to a scale) to $[\mathbf{u}_1]_\times$ when the second and third rows of $\mathbf{K}_{nl}$ and $\mathbf{K}_{nl}$ are chosen the same. In addition, they assumed $\mathbf{K}_{ol}$ = $\mathbf{K}_{or}$ and they were parameterized by a single variable, i.e. focal length. Hence, the fundamental matrix with respect to the Quasi-Euclidean [9] has 7 d.o.f., i.e. 1 for ($\mathbf{K}_{ol}$, $\mathbf{K}_{or}$), 3 for $\mathbf{R}_l'$, and 3 for $\mathbf{R}_r'$.

3. Proposed Method

Inspired by the specific form of fundamental matrices for the rectified coordinates, which remarkably avoids the over-fitting problem in the projective space, we further generalize the image rectification framework to video sequences. Considering the temporal variations and the constraints on the intrinsic parameters, the objective function across all frames can be formulated as follows:

$$E = E_F + \lambda_K E_K + \lambda_t E_t \qquad (4)$$

where E_F , E_K , E_t represent the spatial error energy, internal energy, temporal smoothness energy, respectively, which will be explained subsequently, and (λ_K, λ_t) are the weights used to balance these three energy terms.

The first energy denotes the spatial error cost, which sums the epipolar constraint errors for all the correspondence points in the left and right images via the fundamental matrix $\mathbf{F}$, is given by,

$$E_F\left(K_{ol}^{(t)}, K_{or}^{(t)}, R_{ol}'^{(t)}, R_{or}'^{(t)}\right) = \sum_j \rho_s\left(f_{Samp}\left(\mathbf{F}^{(t)}, \mathbf{m}_l^{j(t)}, \mathbf{m}_r^{j(t)}\right)\right) \qquad (5)$$

The function f_{Samp} is defined as the Sampson error [1] for the j-th pair of correspondence points associated with the fundamental matrix $\mathbf{F}$, given as follows:

$$f_{Samp}\left(\mathbf{F}, \mathbf{m}_l^j, \mathbf{m}_r^j\right) = \frac{\left\|\mathbf{m}_r^{jT}\mathbf{F}\mathbf{m}_l^j\right\|^2}{\left\|\tilde{\mathbf{I}}_3\mathbf{F}\mathbf{m}_l^j\right\|^2 + \left\|\tilde{\mathbf{I}}_3\mathbf{F}^T\mathbf{m}_r^j\right\|^2} \qquad (6)$$

where the matrix $\tilde{\mathbf{I}}_3 = diag(1,1,0)$ is used to indicate the first two entries of the 3-vector. In eq. (5), the robust error function ρ_s is employed to alleviate the influence of outliers, which is given by $\rho_s(r) = \log(1 + r^2 / 2\hat{\sigma}^2)$, known as Lorentzion (or Cauchy) function in robust statistics [10]. Note that the robust standard deviation $\hat{\sigma}$ is

Figure 2. The rectification results on the *hiking* sequence by using the proposed method. Two columns are the left and right views.

self-determined by the order statistics method [11].

The second energy E_K denotes the constraints on the intrinsic parameters in the corresponding camera matrices. The intrinsic parameters of the camera matrix have some reasonable ranges and relations [12], and the imposed constraints on them, e.g. identical focal lengths, zero skew, and principle points close to image center. These constraints are formulated as soft constraints in the function f_K, thus the energy E_K is defined as

$$E_K\left(K_{ol}^{(t)}, K_{or}^{(t)}\right) = f_K\left(K_{ol}^{(t)}\right) + f_K\left(K_{or}^{(t)}\right) \tag{7}$$

The last energy E_t denotes the temporal smoothness constraints on varying intrinsic and extrinsic parameters and is formulated as:

$$\begin{aligned} &E_t\left(K_{ol}^{(t-1)}, K_{or}^{(t-1)}, R_{ol}'^{(t-1)}, R_{or}'^{(t-1)}, K_{ol}^{(t)}, K_{or}^{(t)}, R_{ol}'^{(t)}, R_{or}'^{(t)}\right) \\ &= f_{\delta K}\left(K_{ol}^{(t-1)}, K_{ol}^{(t)}\right) + f_{\delta K}\left(K_{or}^{(t-1)}, K_{or}^{(t)}\right) \\ &+ f_{\delta R}\left(R_{ol}'^{(t-1)}, R_{ol}'^{(t)}\right) + f_{\delta R}\left(R_{or}'^{(t-1)}, R_{or}'^{(t)}\right) \end{aligned} \tag{8}$$

where the functions $f_{\delta K}$ and $f_{\delta R}$ are used to penalize the variations between the current and previous time states.

The Levenberg-Marquardt optimization algorithm with box constraints [13] is applied to solve the nonlinear optimization problem in equation (4). For the first frame, we zero the rotation along the z-axis on the left image to suppress the rectification distortion as well as reduce the ambiguities in the solution. For the subsequent frames, the parameters are initialized by the results of the previous time state.

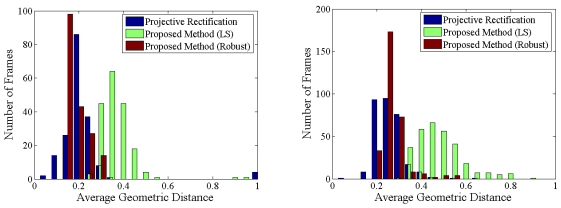

(a) (b)

Figure 3. The histogram of geometric errors in the (a) *walk away* sequence and (b) *hiking* sequence.

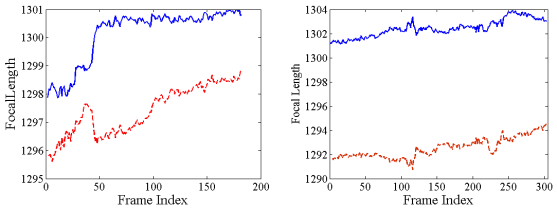

(a) (b)

Figure 4. The curves of the estimated focal lengths in the (a) *walk away* sequence and (b) *hiking* sequence. The blue curves and red dash curves indicate the left and right cameras, respectively.

4. Experimental Results

In our implementation, the box constraints for the first frame are set to within ± 15 degrees in Euler angles and [-1,1] for the focal length parameter α, where $f = 3^{\alpha} \cdot (w+h)$ for image width w and height h [12]. The initial values of all the parameters are set to be zero. For the subsequent frames, the initial values are set to the previous results, and the box constraints for the rotation angles are set to within ± 5 degrees of deviation in Euler angles. We use the above setting for all the experiments in this paper.

All the experiments were performed on the PC with Intel Core2 CPU 6320 of 1.86 GHz 1.87GHz, and DDR RAM 2G. The corresponding feature points were automatically detected and matched via the SIFT feature extraction and matching [14].

We show the experimental results on two stereo sequences, i.e. the *walk away* sequence, as shown in Figure 1, and the *hiking* sequence, depicted in Figure 2. Figure 1 depicts the problem of the conventional projective rectification due to the over-fitting problem in projective space and the significant rectification distortion.

The efficiency of the proposed method is summarized as follows. For the first frame, we set the maximal number of the Levenberg-Marquardt iterations to 200, and it terminated in 2 seconds. For the subsequent frames, the maximal iteration number was set to 20, and it executed at the rate of 2.5-3 fps, depending on the number of match points. Note that the execution time does not include other operations, such as the feature extraction/ matching and image warping.

The histogram of the geometric error distribution is shown in Figure 3. The error measures the average distances of the parallel line of the feature point and its corresponding point on the rectified image pairs. In this figure, we observe the geometric errors of the projective rectification are generally smaller than those of the pro-

Figure 5. The results of stereo matching after applying the proposed rectification algorithm on the video sequences.

posed method. However, the robust estimation (red) of the proposed method has similar error distribution to that of the projective rectification. It is interesting that both methods attempt to minimize the same error, but the error does not directly reflect the rectification distortion. In fact, the proposed algorithm alleviates the undesirable rectification distortion by enforcing the box constraints on the associated camera parameters. Figure 4 shows the variations of the estimated focal lengths.

Finally, we show the results of applying the stereo matching algorithm based on hierarchical belief propagation [15] to the selected frames in the rectified sequences in Figure 5.

5. Conclusions

In this paper, a novel self image rectification algorithm has been proposed for uncalibrated stereo videos with varying camera motion and zooming effects. This method is based on minimizing the geometric constraints over a set of metric camera parameters. In this fashion, the proposed algorithm nicely avoids the over-fitting problem in the projective space. In addition, it alleviates the undesirable rectification distortions. We demonstrate the superior performance of the proposed algorithm over the previous method on two real sequences.

For the future works, we would like to consider the lens distortion into the image rectification algorithm in the same optimization framework. Furthermore, we are also interested in extending this work to intensity consistency or color calibration problems for stereo sequences.

References

[1] R. Hartley, and A. Zisserman. Multiple View Geometry in Computer Vision. Cambridge University Press, Cambridge, UK. 2000.

[2] M. Pollefeys, L. Van Gool, “Self-calibration and metric reconstruction inspite of varying and unknown intrinsic camera parameters”, IEEE Trans. Pattern Analysis and Machine Intelligence, Vol. 21 No. 8, pp. 707 -724. 1999.

[3] R. I. Hartley. “Kruppa’s equations derived from the fundamental matrix”, IEEE Trans. Pattern Analysis and Machine Intelligence, Vol. 19, No. 2, pp. 133-135. 1997.

[4] B. Triggs, “Autocalibration and the absolute quadric”, In Proc. International Conf. on Computer Vision and Pattern Recognition, pp. 609-614. 1997.

[5] Elsayed E. Hemayed. A Survey of Camera Self-Calibration. Proceedings of the IEEE Conference on Advanced Video and Signal Based Surveillance (AVSS’03)

[6] R. I. Hartley. “Theory and practice of projective rectification”, International Journal of Computer, Vol. 35, No. 2, pp. 115–127, 1999.

[7] J. Mallon and P. F. Whelan. Projective rectification from the fundamental matrix. Image and Vision Computing, Vol. 23, No. 7, pp. 643-650, 2005.

[8] Francesco Isgro, Emanuele Trucco, "Projective Rectification Without Epipolar Geometry," IEEE Proc. Computer Vision and Pattern Recognition (CVPR'99) – Vol. 1, pp. 1094, 1999

[9] A. Fusiello and L. Irsara. Quasi-euclidean Uncalibrated Epipolar Rectification. International Conference on Pattern Recognition (ICPR), 2008

[10] G. Li. *Robust regression*. Exploring Data Tables, Trends, and Shapes (D. C. Hoaglin, F. Mosteller and J. W. Tukey Ed.), Wiley, New York, pp. 281--343, (1985).

[11] A. Bab-Hadiashar and D. Suter. Robust segmentation of visual data using ranked unbiased scale estimate. International Journal of Information, Education and Research in Robotics and Artificial Intelligence, vol. 17, pp. 649--660, 1999.

[12] M. Pollefeys, F. Verbiest, and L. Gool. Surviving dominant planes in uncalibrated structure and motion recovery. Proc. European Conf. Computer Vision, 2002.

[13] M. I. A. Lourakis. levmar: Levenberg-Marquardt nonlinear least squares algorithms in C/C++. http://www.ics.forth.gr/~lourakis/levmar/, Jul. 2004

[14] D. G. Lowe, “Distinctive image features from scale-invariant keypoints”, International Journal of Computer Vision, Vol. 60, No. 2, pp. 91-110, 2004

[15] P. F. Felzenszwalb and D. P. Huttenlocher. ?Efficient Belief Propagation for Early Vision.“ In IEEE Proc. CVPR 2004